Three-Dimensional Ion-Beam Lithography in Single-Crystal Diamond

P. Olivero[1,2], F. Picollo[1,2], V. Moi[1], E. Enrico[3], D. Gatto Monticone[1,2], L. La Torre[4], V. Rigato[4], L. Boarino[2], E. Vittone[1,2].

[1] *Experimental Physics Department and "NIS Centre of Excellence", University of Torino, Torino, Italy.*
[2] *INFN Sezione di Torino, Torino, Italy.*
[3] *NanoFacility Piemonte and Quantum Research Laboratory, National Institute of Metrological Research, Torino, Italy.*
[4] *INFN, Laboratori Nazionali di Legnaro, Legnaro (Padova), Italy.*

INTRODUCTION

MeV ion implantation is an effective tool in the micro-fabrication of a vast range of materials [1-5], and in particular it can be effectively adopted to fabricate three-dimensional micro-strucures in single-crystal diamond such as waveguides [6,7], photonic structures [8] and micro-mechanical resonators [9,10]. The damage density can be controlled over a broad range by varying several implantation parameters, such as ion species and fluence, resulting in the formation of point defects, in the amorphization and eventually in the permanent graphitization of the pristine crystal upon thermal annealing when a critical damage threshold is reached [11].

In this structural modification process, high spatial resolution in both lateral and depth dimensions is allowed respectively by the availability of focused ion beams and by the peculiar damage density profile of highly energetic ions in matter. In particular, since most of the ion matter nuclear interaction occurs at the end of implanted ion range, it is possible to define sub-superficial sacrificial layers with high spatial accuracy. In the definition of the lateral features of the structures, complementary techniques such as maskless Focused Ion Beam (FIB) microfabrication [6,8,9] and Reactive Ion Etching (RIE) [7,10] on masked samples have been employed.

In the present paper we report about our first results in the direct fabrication of micro-mechanical structures at the ion microbeam line of the AN2000 accelerator of the Legnaro National Laboratories, in synergy with the FIB instrument available at the "NanoFacility Piemonte" laboratory of the National Institute of Metrological Research (INRiM).

HIGH-ENERGY ION IMPLANTATION

The samples employed in the present work are artificial single-crystal diamonds produced by High Pressure High Temperature (HPHT) technique by Sumitomo Electrics. The samples size is $3\times3\times1.5$ mm^3 and they are classified as type Ib crystals, with typical substitutional nitrogen concentration of 10-100 ppm.

In order to create deep sacrificial layers at defined locations, the samples were implanted with 1.1 MeV He^+ ions at the microbeam line of the AN2000 Van de Graaff accelerator of the Legnaro National Laboratories. 100×100 μm^2 areas were irradiated with a scanning micro-beam in order to deliver a uniform fluence. The damage profile of the above-mentioned ions in the diamond lattice is reported in figure 1, as derived from the SRIM-2008.04 Monte Carlo Simulation code [12] by setting a displacement energy value of 50 eV [13]. The damage profile is derived by assuming a simple linear dependence of the defect density from the implantation fluence, i.e. ignoring complex non-linear processes such as self-annealing and defect-defect interaction. In such a drastically simplified approach it is nonetheless possible to have a satisfactory estimation of the thickness of the buried graphitized layer which is formed upon thermal annealing, by setting a "graphitization" threshold for the vacancy density of $\sim9\cdot10^{22}$ cm^{-3} [11], as shown in figure 1.

The recently implemented system for the monitoring of the implanted charge by using the whole specimen chamber as an electrically insulated "Faraday cup" allowed an accurate fluence control, while the new automatized system for the stage positioning allowed a faster sample processing.

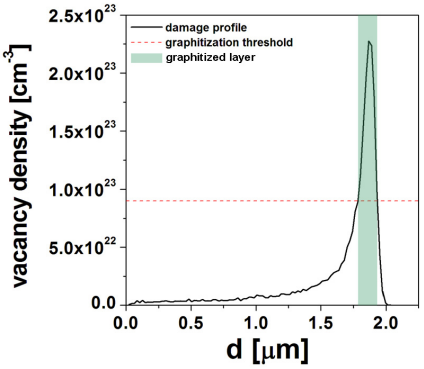

Fig. 1. Damage density profile (black continuous line) for a 1.1 MeV He^+ implantation at a fluence of $1\cdot10^{17}$ cm^{-2}. The graphitization threshold is reported in the dashed line. The graphitized layer formed upon thermal annealing is highlighted in the box.

THERMAL ANNEALING

The implantation was followed by thermal annealing at 950 °C for 2 hours in an inert Ar atmosphere, in order to avoid accidental oxidation of the surface. As mentioned above, the effect of the thermal annealing is to convert the buried amorphized layer to a stable graphitic-like phase

which is prone to selective etching. Figure 2 shows an optical microscopy image in transmission of the sample after thermal annealing. The implanted areas are clearly defined, given the optical opacity of the graphitic layer with respect to the transparent diamond matrix.

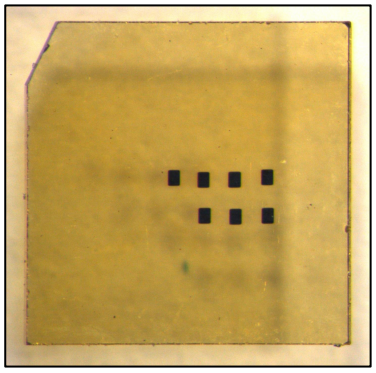

Fig. 2. Optical microscopy image in transmission of the implanted sample after thermal annealing. The 100×100 μm^2 implanted regions are clearly visible.

FIB MICROMACHINING AND SELECTIVE ETCHING

After having defined micro-holes with FIB micromachining for the access of etchants to some of the buried sacrificial layers, the sample was processed with electrochemical etching. The process, consisting in immersing the sample in a weak boric acid solution in presence of strong electrostatic fields applied between Pt electrodes positioned as close as possible to areas of interest, allowed an efficient selective removal of the sacrificial layer. Figure 3 shows a zoomed optical image of the sample after selective etching. The under-etched regions are clearly visible.

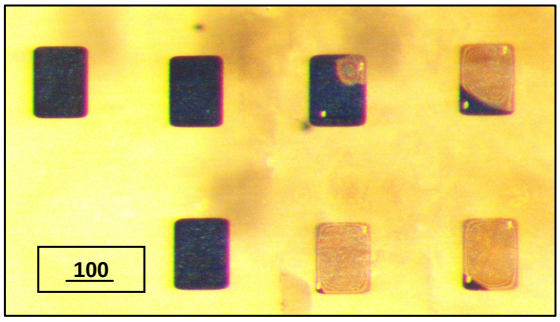

Fig. 3. Optical microscopy image in transmission of the implanted sample after selective graphite etching.

FIB MICROMACHINING AND LIFT-OFF

After the selective etching process provided a complete under-cutting of the areas of interest, FIB micromachining was employed to defined specific portions of the free-standing layer to be lifted-off, as schematically shown in figure 4.

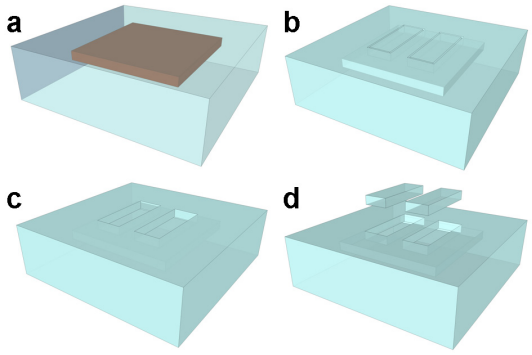

Fig. 4. Schematic representation of the FIB-assisted process for the lift-off of specific regions of the free-standing layer and the definition of three-dimensional structures in the sample.

As shown in figure 5, with the above-described technique it is possible to produce three-dimensional microstructures in single-crystal diamond. Such microstructures have a strong potential in micro-electromechanical (MEMS) and opto-mechanical devices, which are currently under testing in collaboration with the Néel Institute (CNRS, Grenoble).

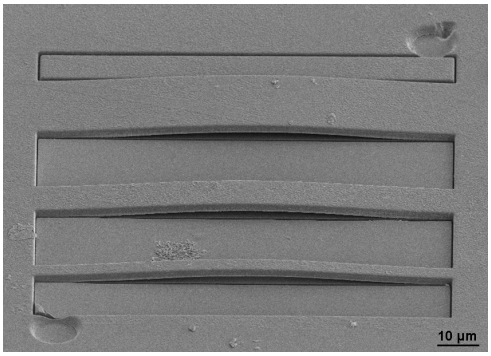

Fig. 5. SEM microscopy image of the final three-dimensional structures in single-crystal diamond.

[1] P. Polesello et al., Nucl. Instrum. Methods Phys. Res. B, 158 (1999) 173.
[2] P. Y. Yang et al., Appl. Phys. Lett., 90 (2007) 241109.
[3] P. Mistry et al., Nucl. Instrum. Methods Phys. Res. B, 260 (2007) 437.
[4] A. Crunteanu et al., Appl. Phys. A, 76 (2003) 1109.
[5] K. Nomura et al., Phys. Rev. B, 68 (2003) 064106.
[6] P. Olivero et al., Adv. Mater., 17 (2005) 2427.
[7] M. P. Hiscocks et al., Diamond Relat. Mater., in press, DOI: 10.1016/j.diamond.2011.02.013.
[8] B. A. Fairchild et al., Adv. Mat., 20 (2008) 4793.
[9] M. Liao et al., Adv. Mat., in press, DOI: 10.1002/adma.201003074.
[10] C. F. Wang et al., J. Vac. Sci. Technol. B, 25 (2007) 730.
[11] P. Olivero et al., Diamond Relat. Mater., 15 (2006) 1614.
[12] J.F. Ziegler et al., Nucl. Instr. Methods Phys. Res. B, 268 (2010) 1818.
[13] D. Saada et al., Int. J. Mod. Phys. C, 9 (1998) 61.